Spectroscopic Characterization of the Interaction of Azide and Thiocyanate with the Binuclear Center of Cytochrome Oxidase: Evidence for Multiple Ligand Sites†

Wenbao Li and Graham Palmer*

Department of Biochemistry and Cell Biology, Rice University, P.O. Box 1892, Houston, Texas 77251-1892

Received August 26, 1992; Revised Manuscript Received December 3, 1992

ABSTRACT: The interactions of azide and thiocyanate with the binuclear center of oxidized cytochrome *c* oxidase have been characterized by Fourier transform infrared and UV–vis spectroscopy, electron paramagnetic resonance and magnetic and natural circular dichroism. Azide binds in two phases, a high-affinity phase (K_d = 64 μM) in which it is bound as a bridge to the binuclear center and a low-affinity phase (K_d = 20 mM) in which it displaces one of the axial ligands to cytochrome *a*. Thiocyanate also binds in two phases. The high-affinity phase (K_d = 2.7 mM) involves binding in a terminal mode to Cu_B; the low-affinity phase is complex and involves both Cu_A and cytochrome *a*. In contrast to the recent proposal of Yoshikawa and Caughey [(1990) *J. Biol. Chem. 265*, 7945–7958], we conclude that cyanide also functions as a bridge between cytochrome a_3 and Cu_B. In the presence of cyanide, azide does not bind to its high-affinity site but thiocyanate does bind to its high-affinity site.

Cytochrome *c* oxidase (CcO)[1] functions as one of the three energy-conserving electron transfer complexes of the mitochondrial electron transport chain. In this capacity it serves both to translocate protons and to connect the electron transport chain with oxygen, the terminal electron-accepting substrate. Thus this enzyme exhibits two chemically distinct but functionally related catalytic activities.

This biological activity of cytochrome oxidase depends minimally upon two copper and two heme A prosthetic groups. One of these copper centers, Cu_A, and one of the heme A centers, cytochrome *a*, serve to conduct electrons from the electron donor, cytochrome *c*, to the catalytic center where dioxygen is reduced to water. This catalytic center contains the two remaining redox-active metal ions, Cu_B and cytochrome a_3; these are believed to be in close proximity and to compose a binuclear center in which oxygen and its reduced intermediates are held as the catalytic cycle is completed.

The crucial consequence of these redox reactions is the preservation of the free energy associated with oxygen reduction via the creation of a transmembrane proton gradient, and it is generally accepted that the transport of protons from the matrix to the intermembrane space is a second fundamental reaction catalyzed by this enzyme. There has been considerable speculation on the site and mechanism of this proton translocation (Gelles et al., 1986), and at one time or another, each of the four redox-active metal centers has been suggested to be responsible for this activity, though there is increasing evidence that the proton translocation process is also implemented at the binuclear center (Wikstrom, 1989).

At the same time data are accumulating that the ligand reactivity of this binuclear center is more versatile was previously suspected; this is particularly true for Cu_B. The following facts all point to such a reactivity: (i) the observations of Alben (1981) on the formation of Cu_B–CO complexes following photodissociation of cytochrome a_3^{2+}–CO, (ii) the response of the oxidized enzyme to nitric oxide (Brudvig et al., 1981), (iii) IR data which suggest that cyanide binds exclusively to Cu_B in oxidized enzyme (Yoshikawa & Caughey, 1990), and (iv) recent kinetic data (Woodruff et al., 1991) which led to the conclusion that gaseous ligands are transiently bound to Cu_B during their passage from the solvent to the heme iron of cytochrome a_3. In addition we have recently suggested (Schoonover & Palmer, 1991) that the fast-to-slow conformational change exhibited by this enzyme (Baker et al., 1987) is the result of a change in coordination which occurs at this copper center.

Most of the proposed mechanisms for the translocation of protons by this enzyme are essentially extensions of the redox Bohr concept in which the proton and/or metal affinity of acidic or basic ligands changes with changes in the oxidation state of one of the redox-active metal ions. Consequently, the possibility of facile ligand reactivity at a participating metal center becomes of considerable interest.

In pursuing both this topic and our continuing interest in the structural origins of the fast-to-slow transition, we have sought to use the vibration spectra of infrared-active metal ligands as a potential tool to further characterize the properties of selected small molecules as they are bound to cytochrome oxidase. Infrared spectroscopy has previously been used to investigate the binding of carbon monoxide and cyanide to cytochrome oxidase (Yoshikawa & Caughey, 1982, 1990). We have now found that FTIR spectroscopy is a useful method for investigating the interaction of azide and thiocyanate to this enzyme and have obtained evidence for two sites, of quite distinct reactivity, which can be simultaneously occupied by different ligands in the fully oxidized enzyme. Yoshikawa and Caughey (1992) have also studied the interaction of azide with cytochrome oxidase using the IR technique.

MATERIALS AND METHODS

CcO was prepared by the modification of the method of Hartzell and Beinert (1974) developed in this laboratory

† Supported by grants from the National Institutes of Health (GM 21337) and the Welch Foundation (C636).

* Corresponding author.

[1] Abbreviations: CcO, cytochrome *c* oxidase; FTIR, Fourier transform infrared; HEPES, 4-(2-hydroxyethyl)-1-piperazineethanesulfonic acid; DM, dodecyl maltoside; EDTA, (ethylenedinitrilo)tetraacetic acid, disodium salt; EPR, electron paramagnetic resonance; (M)CD, (magnetic) circular dichroism; SOD, superoxide dismutase; Mb, metmyoglobin; Cyt.c, cytochrome *c*; CT, charge transfer; HALS, highly anisotropic low spin; EXAFS, extended X-ray absorption fine structure; FWHH, full width at half-height.

0006-2960/93/0432-1833$04.00/0

(Baker et al., 1987). This procedure routinely gave enzyme which reacts in a single rapid phase with cyanide. The absorbance maximum in the Soret was at 423–424 nm.

CcO was first passed down a Bio-Rad 10-DG desalting column equilibrated with HEPES–DM to remove residual ammonium sulfate following preparation. Subsequently the enzyme was exchanged into D_2O buffer prepared by dissolving lyophilized aqueous HEPES–DM in an equal volume of D_2O. Exchange was achieved by 3–4 cycles of concentration and dilution using Amicon Centriflo ultrafiltration cones centrifuged at 4000 rpm for 30 min in a Beckman J20 rotor with the final centrifugation yielding enzyme of about 0.6–0.7 mM enzyme (aa_3 basis).

Aliquots of enzyme were treated with ligand solution or an equal volume of D_2O buffer. The protein was loaded into a FTIR cell of 0.05-mm path length; the windows were CaF_2 and the path length was established with a Teflon spacer. In some experiments the D_2O content of the enzyme was determined using the infrared absorption of H_2O at 1655 cm^{-1} and reference to a standard curve prepared using known mixtures of H_2O in D_2O. The free ligand solution was then prepared in a solvent of the same composition. Data consisted of 512 coadded interferograms usually recorded with 2-cm^{-1} spectral resolution. Interferograms were obtained on buffer ± ligand and CcO ± ligand. The total concentration of ligand was the same in both cases. The FTIR spectrum of the free ligand was subtracted from that of the enzyme–ligand mixture, using the calculated amount of bound ligand (see Results) to weight the amount of free ligand spectrum to be subtracted. In practice this value was adjusted slightly to minimize negative features in the difference spectrum. These adjustments did not exceed ±15% of the initially calculated value. Finally, the spectra were subjected to baseline correction so that the baseline was flat over the spectral range of interest. All of these manipulations were carried out using the software provided with the FTIR spectrometer (Mattson Galaxy 6020 equipped with liquid nitrogen-cooled MCT detector). The final spectra were usually analyzed using a curve-fitting package provided with IGOR, a graphing and data analysis package for the Macintosh (Wavemetrics, Oregon). Both Lorentzian and Gaussian lines were routinely tested; it was routinely observed that Gaussian line shapes yielded better fits.

Optical spectra on the enzyme samples used in the FTIR experiments were recorded directly in the FTIR cuvette using a cell holder designed for the Cary 17. Other absorbance measurements were made in an IBM 9430 spectrophotometer. EPR spectra were obtained using a Varian E-line spectrometer operating at 12 K. CD and MCD spectra were obtained on a Jasco-500C spectrometer equipped with a 1.3-T electromagnet; for near-IR measurements a red-sensitive detector and fixed slits of 200 μm were employed. All instruments were interfaced to microcomputers for data storage and analysis.

Cytochrome *c* (Type VI) and horse heart myoglobin were purchased from Sigma and bovine liver superoxide dismutase from DDI Pharmaceuticals (Mountain View, CA). The superoxide dismutase was dialyzed vs 15 volumes of 10 mM EDTA in 0.1 M potassium phosphate, pD 8.2, prepared in 99.9% D_2O (Cambridge Isotope Laboratories), followed by two changes of the same buffer without EDTA; the SOD concentration was determined from the absorbance at 258 nm using A_m = 10 300 M^{-1} cm^{-1} (McCord & Fridovich, 1969). The cytochrome *c* and myoglobin were used as supplied, the myoglobin being filtered through a 0.42-μm filter to remove some insoluble material. Nonisotopically labeled thiocyanate and selenocyanate were recrystallized from hot water and 5:1 ethanol–water, respectively. Azide was recrystallized from ethanol; no difference from unrecrystallized azide was found. Isotopically labeled azide was purchased from ICON (Mt. Marion, NY) and isotopically labeled thiocyanate from Cambridge Isotope Laboratories. They were used as supplied.

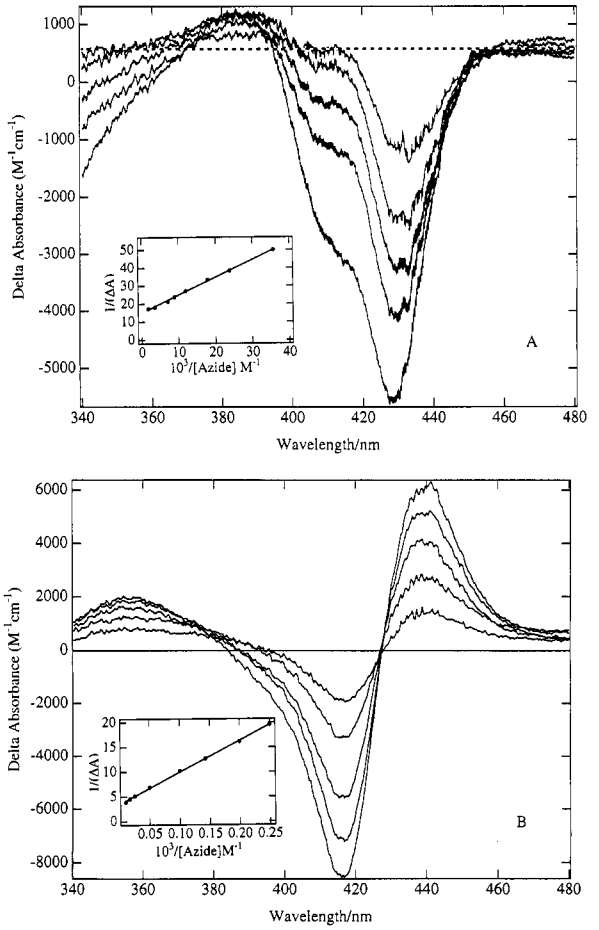

FIGURE 1: Difference spectra of CcO–azide *minus* CcO. The buffer was 50 mM HEPES + 0.1% DM, pH 8.0, and the temperature was 25 °C. All spectra were recorded in a 1-cm path length cell with a time constant of 1 s. (A) The spectra shown were computed from the absolute spectra of a 7.0 μM CcO solution in the absence and following addition of azide (20, 50, 100, and 200 μM and 1 mM). All spectra were corrected for dilution. The inset shows the double-reciprocal plot of absorbance decrease at 429 nm versus azide concentration yielding a K_d = 64 μM. The average of four experiments was 65 μM. (B) The spectra shown were computed from the absolute spectra of a 6.2 μM CcO solution in the presence of 1 mM azide and following addition of azide to a final concentrations of 3.5, 6, 11, 16, and 21 mM. The inset shows the double-reciprocal plot of absorbance at 439–416 nm versus total azide concentration yielding a K_d = 20 mM. The average value was 21 mM.

RESULTS

Effect of Azide Binding on the Absorption Spectrum. Addition of sodium azide to fast CcO leads to two series of absorbance changes. With azide concentrations below 1 mM the observed changes consist principally of small decreases in the Soret absorption which are most easily visualized as difference spectra calculated with respect to untreated enzyme. The difference spectra (Figure 1A) exhibit a trough at 429 nm, an inflection at 410 nm, a peak at 385 nm, and a zero crossing at 397 nm. A double-reciprocal plot of the absorbance decreases at 429 nm versus azide concentration is linear (Figure 1A, inset) and yields values of 64 μM for the dissociation

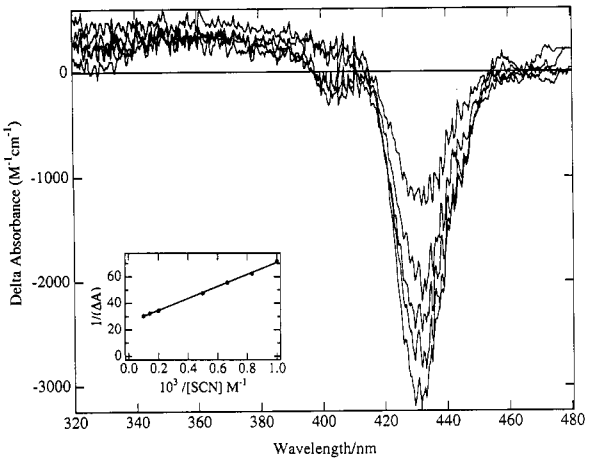

FIGURE 2: Difference spectra of CcO–SCN *minus* CcO. All conditions were as described for Figure 1. The spectra shown were computed from the absolute spectra of a 6.5 μM CcO solution in the absence and following addition of thiocyanate (2, 4, 6, 10, and 15 mM). All spectra were corrected for dilution. The inset shows the double-reciprocal plot of absorbance decrease at 431 nm versus thiocyanate concentration yielding a K_d = 2.7 mM.

constant and 5800 M^{-1} cm^{-1} for the maximum absorbance decrease. We refer to this reaction as the high-affinity phase.

With azide concentrations above 1 mM the form of the difference spectra changes. To study these changes the difference spectra were calculated with respect to enzyme treated with 1 mM azide; at this concentration the high-affinity changes are essentially complete. The observed spectra (Figure 1B) exhibit a bilobed pattern with a minimum at 416 nm and a maximum at 439 nm, implying that the Soret maximum has become red-shifted; weak positive absorbance is present below 398 nm. An isosbestic point is present at 427 nm; occasionally some deviation from isosbestic behavior is observed at the lowest concentration of azide, presumably signifying some residual effect of the high-affinity phase. A double-reciprocal plot (Figure 1B, inset) is again linear and yields a K_d of 20 mM and a maximum absorbance excursion (439–416 nm) of 3.2 × 10^4 M^{-1} cm^{-1}. We call this the low-affinity phase.

There were no obvious changes in the α-band or at 830 nm at any azide concentration. However, the 655-nm shoulder responded differently during the high- and low-affinity phases. These changes were most easily detected by MCD (see below).

Effect of Thiocyanate Binding on the Absorption Spectrum. When the above experiments were repeated with sodium thiocyanate, well-behaved data were only obtained at moderately low concentrations of ligand (Figure 2); the spectral changes were generally similar in shape to those observed during the high-affinity azide changes. A K_d of 2.7 mM could be extracted from the linear double-reciprocal plot of the absorbance changes at 431 nm versus the concentration of thiocyanate; the extrapolated absorbance decrement was 3400 M^{-1} cm^{-1}. Above 50 mM SCN the observed changes in the optical spectrum became complex with additional absorbance decreases changing to absorbance increases as the concentration of thiocyanate was raised to 0.2 M. Small decreases were seen at 830 nm; for example, 0.25 M SCN led to a 25% loss in the amplitude of the 830–720-nm difference absorbance. Small changes were also apparent in the α-band and at 655 nm (see below).

Repetition of these experiments with potassium selenocyanate led to a difference spectrum similar to that obtained upon addition of sodium cyanide to CcO, with a minimum at 413 nm, a maximum at 433 nm, and a zero crossing at 424 nm; a double-reciprocal plot of the absorbance changes gave an apparent K_d of 2.5 mM. However, as the rate of binding of selenocyanate to CcO was slow, this value must be considered approximate. When the same solution of selenocyanate was reacted with metmyoglobin a small absorbance decrease together with a shift of the Soret maximum from 409 to 411 nm was detected. No evidence for formation of the metmyoglobin cyanide derivative with its maximum at 423 nm could be found even though the affinity of myoglobin for cyanide is high and the reaction was studied for 18 h. We find the K_d of CN for Mb to be 1 μM, confirming the earlier result of Sono and Dawson (1982). It thus seems unlikely that the changes observed with CcO are due to a cyanide contamination in the KSeCN. Identical results were obtained with freshly recrystallized KSeCN.

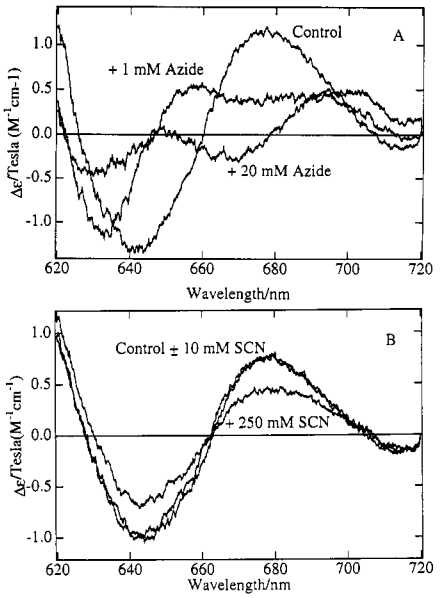

FIGURE 3: Comparison of the near-IR MCD spectra of CcO reacted with either azide or thiocyanate. The spectra are the average of four scans using a red-sensitive detector and fixed slits of 200 μm. All sample concentrations were approximately 100 μM; other conditions were as described for Figure 1. (A) Spectra of CcO alone and with 1 and 20 mM azide. (B) Spectra of CcO alone and with 10 and 250 mM SCN.

MCD Spectra. With the exception of the wavelength range of 620–720 nm the addition of azide or of thiocyanate to CcO did not lead to any striking changes in the MCD spectrum. However, clear changes were observed in this near-infrared region. With fast CcO the MCD spectrum in this region consists of a positive apparent A-term centered at 660 nm which is assumed to be associated with the 655-nm shoulder present in the absorbance spectrum. From model compounds it is known that this absorbance transition is due to high-spin heme A, which in the case of CcO is present in cytochrome a_3; there is some evidence that the properties of this band may be modified by the interaction with Cu_B (Mitchell et al., 1991). Low concentrations of azide (1 mM) lead to a blue shift of this transition with the zero crossing moving to 645 nm while a positive feature remains at 700 nm (Figure 3A). The corresponding absorption spectrum show a decrease in the prominence of the 655-nm shoulder, presumably as a result of this band moving closer to the much more intense 600-nm absorption of cytochrome *a*. With 10 mM NaSCN the 660-nm MCD band is almost unaffected, the differences being within the noise of the data (Figure 3B); the corresponding absorbance spectra show almost no change (when unrecrystallized SCN was used, small blue shifts (about 5 nm) were observed with little or no change in intensity).

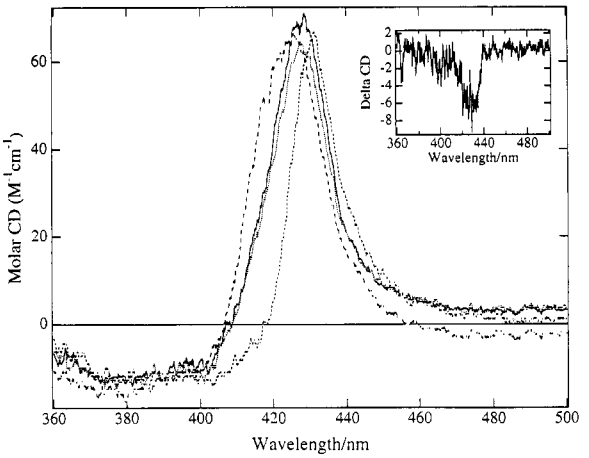

FIGURE 4: Effect of several ligands on the CD spectrum of CcO in the Soret regions. The spectra of CcO (—), CcO with 1 mM azide (···), CcO with 10 mM cyanide (- - -), and CcO with 100 mM formate (– – –). The enzyme concentration was 6.5 μM throughout; the buffer was 50 mM HEPES + 0.1% DM, pH 8.0. The Soret CD spectra are the average of eight scans using a fixed spectral bandwidth of 2 nm and a time constant of 1 s; the path length was 1 cm. The inset shows the difference CD spectrum of CcO + 1 mM azide *minus* CcO.

With higher concentrations of sodium azide the near-IR MCD band red-shifts; for example, with 20 mM azide the zero crossing moves to 675 nm and two positive MCD transitions become apparent, one centered at 645 nm and the second at 700 nm (Figure 3A). These additional changes are not observed with concentrations of SCN as high as 250 mM, though a small decrease in MCD intensity is apparent (Figure 3B).

Addition of SeCN to CcO produces much more extensive changes. In particular, there is a doubling in the intensity of the Soret MCD band centered at 427 nm, similar to that observed when CcO is incubated with cyanide (Babcock et al., 1976).

CD Spectra. The CD spectrum of CcO is dominated by a single positive Cotton effect at 428 nm (Figure 4), as originally observed by Myer (1971). Upon addition of 1 mM azide there is a small decrease in intensity which leads to the difference spectrum shown in Figure 4 (inset). Addition of 10 mM cyanide to CcO leads to a net red shift, the maximum now occurring at 431 nm; subsequent addition of azide did not produce any further change. Conversely, addition of 0.1 M formate to CcO leads to a net blue shift with a maximum at 425 nm. In each case there is weak negative CD below about 400 nm. Addition of 10 mM SCN had no detectable effect on the observed CD spectrum of CcO.

EPR Spectra. Addition of low concentrations of either azide or thiocyanate to fully oxidized CcO did not produce any clear changes in the EPR spectrum between 200 and 4200 G, though a small decrease in the amplitude of the g = 3 signal of cytochrome *a* in the presence of azide was noted. However, high concentrations of both reagents led to clear changes in the low-spin $g = 3$ signal associated with cytochrome *a*. With azide the g = 3 signal loses intensity and acquires a slight inflection on the low-field side and a new EPR signal appears at g = 2.6 (Figure 5A). As the g-value(s) of these low-spin EPR signals is governed by the identity of the ligands attached to the axial coordination sites of cytochrome *a*, it is clear that high concentrations of azide displaces one of the endogenous histidine ligands present at the heme iron of this redox center. The g-value of 2.6 seen with high concentrations of azide is typical of proteins having histidine–azide axial

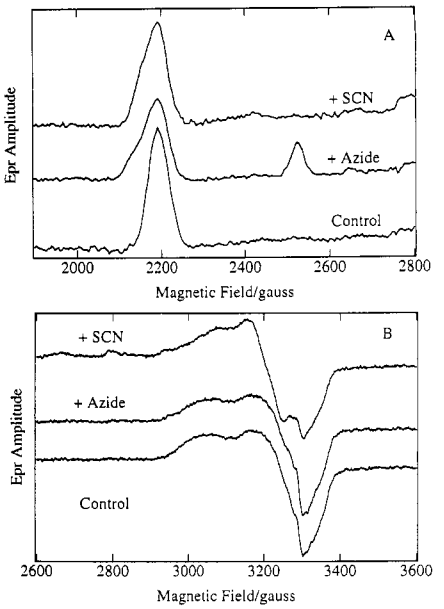

FIGURE 5: Comparison of EPR spectra of CcO (bottom), CcO with 20 mM azide (center), and CcO with 250 mM thiocyanate (top). Data were recorded at 1 mW at 12 K and at 3 mW at 80 K; the modulation amplitude was 20 G. (A) Spectra recorded at 12 K. Enzyme concentration was approximately 60 μM. (B) Spectra recorded at 80 K. Enzyme concentration was approximately 100 μM.

Table I: Infrared Frequencies and Line Widths[a] for Azide[b]

	$^{14}N_3$	$^{15}N_3$	shift	^{15}N splitting
free	2043 (20)	2033 (19)	10	
Mb	2042 (10)	2040 (10)	2	
		2025 (7)	17	15
	2021 (9)	2018 (12)	3	
		2002 (10)	19	16
Cyt.c	2034 (18)	2023 (24)[c]	11	
SOD	2056 (14)	2047 (16)[c]	9	
CcO	2051 (9)	2045 (9)	6	
		2036 (8)	15	9
	2039 (5)	2022 (5)	17	

[a] The full width at half-height values are shown in parentheses. [b] Gaussian fits, except as noted. [c] One-peak fit.

ligation (Blumberg & Peisach, 1971). With 250 mM SCN there is also a slight loss in amplitude at g = 3 but this is principally due to a small increase in the width of the peak. Changes in line shape at high ionic strength have been reported previously (Hartzell & Beinert, 1974).

Azide concentrations up to 50 mM had no clear effect on the EPR signal of Cu_A; higher concentrations were not examined. Concentrations of SCN below 20 mM also do not affect Cu_A, but above 50 mM SCN marked changes in the line shape of Cu_A can be seen (Figure 5B), suggesting a significant change in coordination of this metal center at these high concentrations.

FTIR Spectra of Azide. The infrared spectrum of sodium azide exhibits an asymmetric stretch at 2043 cm^{-1} in D_2O. With sodium azide terminally labeled with ^{15}N the peak position shifts to 2033 cm^{-1} without any change in width (Table I).

When 0.7 mM CcO is treated with 1 equiv of sodium azide approximately 74% of the enzyme is converted to the high-affinity azide complex. This derivative exhibits a single infrared absorption at 2051 cm^{-1} which is substantially narrower than that observed with free azide (Figure 6; Table I). Upon repeating the experiment with azide terminally labeled with ^{15}N we find the frequency of the IR mode to be

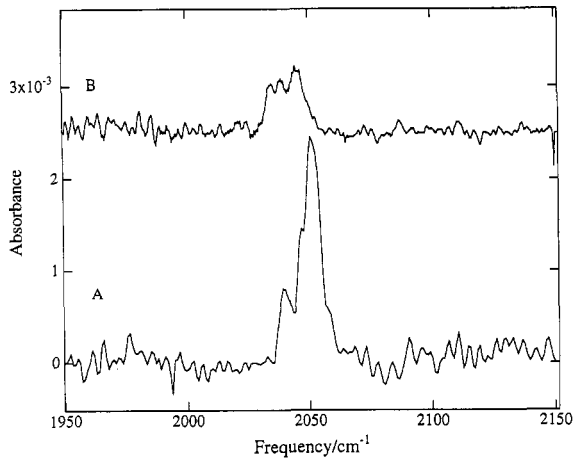

FIGURE 6: FTIR spectra of CcO with 1 equiv of sodium azide; the buffer was 50 mM HEPES + 0.1% DM, pD 8.2. The reference cell for each measurement contained the same concentration of CcO. (A) 0.7 mM CcO + 0.7 mM N_3, represents an average of 512 scans at 2-cm^{-1} resolution. (B) 0.7 mM CcO + 0.7 mM $^{15}N_3$, represents an average of 1024 scans at 1-cm^{-1} resolution. The spectrum has been displaced along the vertical axis.

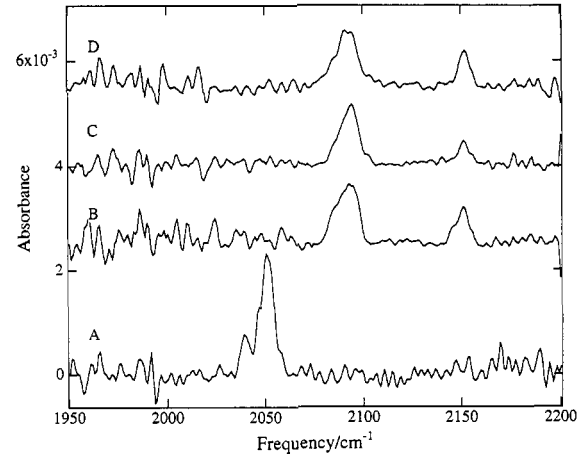

FIGURE 7: Comparison of FTIR spectra of CcO with 1 equiv of azide in the absence and presence of 10 mM cyanide; the buffer was 50 mM HEPES + 0.1% DM, pD 8.2. The reference cell for each measurement contained the same concentration of CcO. All spectra represent an average of 512 scans at 2-cm^{-1} resolution. The spectra have been displaced along the vertical axis. (A) 0.6 mM CcO + 0.6 mM azide; (B) 0.6 mM CcO + 10 mM CN for 15 min and then + 0.6 mM azide for 15 min; (C) 0.6 mM CcO + 0.6 mM azide for 15 min and then + 10 mM CN for 1 h; (D) 0.6 mM CcO + 10 mM CN for 1 h.

lowered to 2038 cm^{-1}. In this case the absorption envelope is clearly broadened with respect to that obtained when the isotopically normal ligand is bound to CcO (Figure 6). To accurately measure the width of this spectrum it is crucial that the spectrum of free ligand be obtained in the same percentage of D_2O as that of the enzyme. For example, the difference between the spectrum of free azide recorded in 75% D_2O and that recorded in 100% D_2O is a peak at 2049 cm^{-1} with a FWHH of 14 cm^{-1}; for ^{15}N azide the corresponding values are 2039 and 14 cm^{-1}. These difference features lie sufficiently close to those of the enzyme-bound azide as to obscure the true line shape of the bound ligand (this problem did not occur with SCN, the relevant difference spectrum being found at 2076 cm^{-1}, well away from the enzyme–SCN mode; see below).

By quantifying the amount of D_2O present in the enzyme as described in Materials and Methods it was possible to exactly match the D_2O in both free and bound azide samples. With this precaution the spectrum of bound ^{15}N azide shown in Figure 6 was obtained; the overall half-width of the IR absorption had increased to 18 cm^{-1}. Fitting the data with two Gaussian curves yielded peaks at 2036 and 2045 cm^{-1} which were of comparable intensity and half-width (8 and 9 cm^{-1}, respectively).

At the equimolar ratio of enzyme and azide a second weaker feature is observed at 2039 cm^{-1} (Table I); this minor species accounts for approximately 10% of the total FTIR intensity. From the K_d of the low-affinity phase about 5% of the low-affinity site is expected to be occupied at these concentrations. Upon increasing the ratio of azide to CcO the intensity of the minor species at 2039 cm^{-1} increases rapidly, with relatively small changes in the size of the mode at 2051 cm^{-1}. However, the difficulties in accurately compensating for the contributions of the unbound ligand and the complications arising through slight mismatches in the D_2O content are exacerbated. Consequently, obtaining reliable quantitative results becomes much more difficult.

CcO treated with 10 mM cyanide for 15 min shows two IR features; these are located at 2092 and 2151 cm^{-1} (Figure 7). The lower frequency component is due to free, residual HCN and the higher frequency component to cyanide bound to CcO (Yoshikawa & Coughey, 1990). Treatment of cyanide-reacted enzyme with azide at a 1:1 ratio did not give a line at 2051 cm^{-1} even after prolonged incubation; direct absorbance measurement of the sample while present in the FTIR cell clearly showed that the Soret maximum had shifted from 423 nm, the wavelength characteristic of both the native enzyme and its azide derivative, to 428 nm, the wavelength characteristic of the cyanide derivative of cytochrome oxidase. Likewise, when 1:1 azide–CcO in which the 2051-cm^{-1} band is fully developed is treated with 10 mM cyanide for 1 h, the IR peak at 2051 cm^{-1} disappears and only the bands at 2092 and 2151 cm^{-1} due to cyanide can be observed; again the Soret maximum is located at 428 nm. Thus, while cyanide was able to displace azide, it was not possible to displace cyanide with azide.

A different result is obtained when formate is used in place of cyanide. Treatment of CcO with formate either before or after addition of azide does not affect the formation of an IR mode at about 2050 cm^{-1} while the absorbance changes typical of formate binding (a shift of the Soret maximum to 418 nm) are clearly obtained. When azide is added to enzyme pretreated with formate the amplitude of the optical and CD changes in the Soret are about 1% of the total signal, though some similarities to Figure 1A can be noted.

Because it has been suggested that azide present in non-metal sites might exhibit a modified IR spectrum (Yoshikawa & Caughey, 1992), we have examined the effect of 1 mM serum albumin on the FTIR of 1 mM azide; no new infrared modes could be detected.

FTIR of Thiocyanate. The infrared spectrum of sodium thiocyanate exhibits an asymmetric C–N stretch at 2064 cm^{-1} (Table II). With sodium thiocyanate labeled with ^{15}N the peak position shifts to 2037 cm^{-1}, with essentially no change in the width of the absorption envelope (Table II), while with sodium thiocyanate labeled with ^{13}C the peak position shifts to 2016 cm^{-1}, again with no change in the width of the absorption envelope (Table II).

When 0.65 mM CcO is treated with 10 mM NaSCN approximately 78% of the enzyme is converted to the high-affinity SCN complex. This derivative exhibits a single weak, infrared mode at 2041 cm^{-1} which is somewhat narrower than that observed with free SCN (Figure 8; Table II); the apparent asymmetry in line shape is an artifact of data processing and

Table II: Infrared Frequencies and Line Widths[a] for Thiocyanate[b]

	SCN	$SC^{15}N$	shift	$S^{13}CN$	shift
free	2063 (37)	2037 (36)	26	2016 (37)	47
Mb	2003 (22)	1977 (20)	26	1956 (24)	47
	2045 (28)	2020 (26)	25	1994 (29)	51
Cyt.c	2048 (27)	2025 (27)	23	2000 (29)	48
SOD	2050 (28)	2025 (26)	25	*c*	
CcO (10 mM SCN)	2041 (23)	2016 (24)	25	1997 (29)	44
CcO (250 mM SCN)	2042 (24)	2015 (23)	27	1996 (25)	46
	2089 (14)	2064 (16)	25	2039 (15)	50

[a] The full width at half-height values are shown in parentheses. [b] Gaussian fit. [c] Not determined.

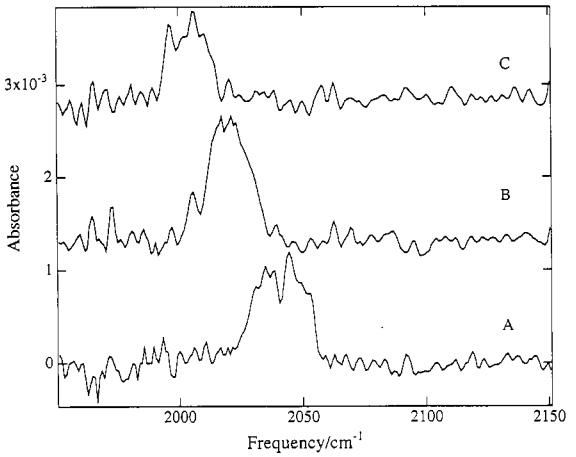

FIGURE 8: FTIR spectra of 0.65 mM CcO with 10 mM thiocyanate in pD 8.2 buffer. The conditions of FTIR are described in Figure 7. (A) CcO + SCN; (B) CcO + $SC^{15}N$; (C) CcO + $S^{13}CN$.

could not be seen in the raw data. Upon repeating the experiment with $SC^{15}N$ we find the IR mode to be lowered to 2016 cm^{-1} with no further decrease in the width of absorption envelope. Repeating the experiment with $S^{13}CN$ gave a peak at 1997 cm^{-1} with an apparent increase in width [carbon shifts are usually bigger than nitrogen shifts (Table II)]. At 250 mM SCN all peaks shift to higher values (Table II). As noted above, this high concentration leads to a large distortion of the EPR spectrum of Cu_A; the new IR frequencies are substantially higher than those seen with SOD and Mb (Table II).

FTIR spectra of CcO–azide, CcO–$SC^{15}N$, and CcO–azide–$SC^{15}N$ are shown in Figure 9. ^{15}N-Labeled SCN was used to increase the separation of the SCN and azide modes. Assuming independent sites, we calculate that 72% of CcO was complexed with azide and 78% with SCN. The presence of azide had no obvious effect on the IR modes characteristic of SCN and, likewise, the presence of SCN had no effect on the IR modes of azide.

Addition of 25 mM SCN (leading to 90% saturation) to enzyme pretreated with 10 mM cyanide for 15 min still led to the appearance of the SCN mode at 2041 cm^{-1} while the characteristic cyanide mode at 2151 cm^{-1} is unaffected (Figure 10). Thus, both SCN and cyanide can be bound to CcO at the same time (at this concentration of SCN a small amount of the Cu_A–SCN mode at 2090 cm^{-1} is present). Again, the absorbance decreases following addition of thiocyanate were very small and it appeared that the order of addition was important, larger changes being found when thiocyanate rather than cyanide was added first; in this latter instance the difference spectrum resembled that of Figure 2 though with only 60% of the amplitude.

FTIR of Ligand Complexes of Myoglobin, Cytochrome c, and Superoxide Dismutase. As part of our attempt to understand these results we have obtained similar spectroscopic data on two heme-containing proteins, myoglobin and cytochrome *c*, and a copper-containing protein, superoxide dismutase. The infrared data are collected in Tables I and II. When more than one value is reported, the result is from a multicomponent fit in which the widths of each component are required to be comparable. Fits which led to two components of substantially different widths were discounted. The results obtained with Mb–azide are similar to those published previously by Caughey (1980).

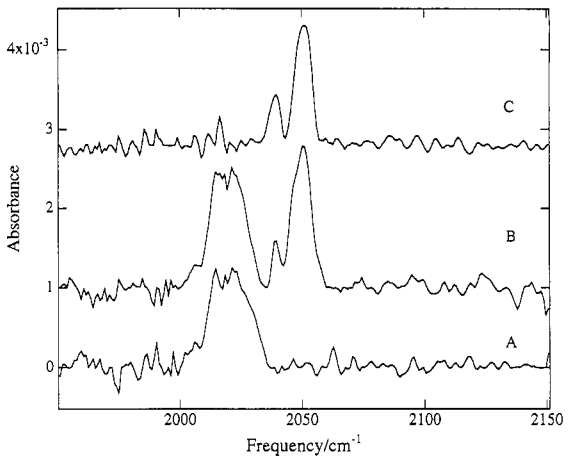

FIGURE 9: Comparison of FTIR spectra of 0.6 mM CcO with 1 equiv of azide and 10 mM thiocyanate in pD 8.2 buffer. The conditions of FTIR are described in Figure 7. (A) CcO + 10 mM $SC^{15}N$ for 15 min; (B) CcO + 10 mM $SC^{15}N$ for 15 min and then + 0.6 mM azide for 15 min; (C) CcO + 0.6 mM azide.

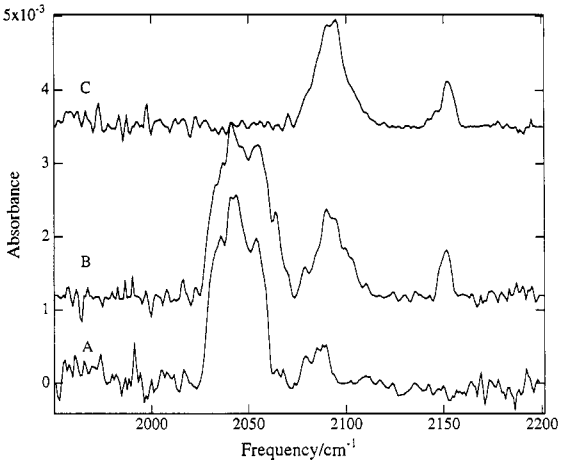

FIGURE 10: Comparison of FTIR spectra of 0.68 mM CcO with 25 mM thiocyanate and 10 mM cyanide in pD 8.2 buffer. The conditions of FTIR are described in Figure 7. (A) CcO + 25 mM SCN; (B) CcO + 10 mM CN for 15 min and then 25 mM SCN; (C) CcO + 10 mM CN.

The values of SOD shown in Table II are for enzyme which had been dialyzed. Undialyzed enzyme shows a second peak at 2080 cm^{-1}; as copper sulfate plus excess sodium thiocyanate exhibits an IR peak at 2060 cm^{-1}, the peak at 2080 cm^{-1} may reflect adventitious copper present in the sample.

EPR Spectra of Azide and Thiocyanate Complexes of Cytochrome c and Myoglobin. The EPR spectra of cytochrome *c* treated with high concentrations of azide (Ikeda-Saito & Iizuka, 1975) or thiocyanate show marked changes consistent with the displacement of the axial methionine by these agents. Upon addition of 0.05 M azide the g_z = 3.06 low-field feature of native cytochrome *c* is shifted upfield to 2.75 and 2.69, while addition of 0.5 M SCN shifts g_z downfield

to 3.4. The data with azide differ somewhat from that published previously (Ikeda-Saito & Iizuka, 1975), where only a single feature at $g = 2.73$ was observed. We have found the splitting with batches of cytochrome *c* obtained at different times and with a sample from a second vendor (Fluka). It is present at all pH values between 6 and 8 and is unchanged whether we used freshly recrystallized azide or solutions which are several weeks old. The corresponding high-field *g*-values (g_x) were 1.75 and 1.79; g_y was 2.25 in both cases.

The 695-nm band of cytochrome *c* characteristic of heme methionine coordination is affected by concentrations of azide larger than 10 mM being about 50% reduced by 100 mM azide and almost totally eliminated by the presence of 1 M azide; the K_d for azide was estimated to be 116 mM. From observations on the decrease of the 695-nm band with increasing concentrations of SCN, the K_d for SCN binding to cytochrome *c* was estimated to be over 1 M.

The optical and EPR properties of myoglobin–azide derivatives have been well characterized (Sono & Dawson, 1982); our data confirm their results.

Addition of large concentrations of SCN to horse Mb led to a small red shift of the Soret from 409 to 411 nm. There was a parallel increase in MCD intensity in the Soret consistent with an increase in low-spin content which was apparent in the EPR as a feature at $g_z = 3.4$, slightly upfield from MbCN. More than half of the myoglobin was still high-spin in the presence of 250 mM SCN. Interestingly, the data with horse and whale Mb were different, the whale protein exhibiting a much larger contribution of a second low-spin feature at 2.63, 2.32, and 1.77 which was barely evident with the horse protein. This second species has previously been reported by Sono and Dawson (1982), also using the whale protein; these workers made measurements at liquid nitrogen temperatures, which undoubtedly is the reason that they did not detect the signal at $g = 3.4$. This EPR feature of MbSCN is close to that of MbCN; with cytochrome *c* the low-spin EPR is found at 3.36. These values are typical of HALS species (Palmer, 1985). In the presence of SCN Mb also shows a large high-spin EPR signal at $g = 6$, and it seems likely that the stretch at 2045 cm^{-1} arises from the low-spin Mb–SCN and the stretch at 2003 cm^{-1} arises from high-spin Mb–SCN. At room temperature MCD shows that Mb–SCN is mainly in the high-spin form; a rough estimate suggests that only 20% of the heme is low-spin.

DISCUSSION

The azide anion has been widely used as a probe of metal sites in both heme- and copper-containing proteins. For those heme proteins which are able to exist in both high-spin and low-spin forms, azide exhibits a relatively strong ligand field. For example, with ligand complexes of myoglobin and leghemoglobin, azide is comparable to pyridine in its ability to convert these proteins to the low-spin form, the series of effectiveness being CN > imidazole > pyridine ~ azide ~ thiocyanate (Vickery et al., 1976; K. Carter, G. Palmer, J. Wittenberg, and C. A. Appleby, unpublished data).

Thus it has always been surprising that addition of azide to CcO leads to such small changes in the optical spectrum (Figure 1). Under the conditions of the high-affinity phase there is a barely detectable decrease in absorbance in the Soret region together with a slight blue shift in the 655-nm feature. Similar small changes had been noted previously (Wever et al., 1973; Nicholls et al., 1976), but our data are somewhat in disagreement with the earlier work. Wever et al. (1973) found that the spectral changes consisted of a blue shift in the Soret maximum, behavior which we have never observed. This blue shift is in fact reminiscent of that which occurs during the fast-to-slow transition and we suspect that it is this process that is complicating the results observed earlier. The fast-to-slow conversion is promoted by low pH and by high detergent (Baker et al., 1987), though with our preparation of CcO the fast-to-slow conversion would not have occurred during the short time presumably needed by Wever et al. to conduct their experiments. To complicate matters, Nicholls et al. (1976) report spectral changes which, while qualitatively similar to those described by Wever et al. (1973), exhibit striking quantitative differences. Nicholls' data are most simply understood if they consist of a mixture of both the high- and low-affinity phases that we document; such a mixture would have the effect of attenuating the amplitude of the extrema present at 415 and 432 nm observed by Wever et al. by difference spectroscopy. If true, this conclusion implies that the cytochrome *a* component present in the preparation of cytochrome oxidase utilized by Nicholls et al. was more readily attacked by azide (see below) than is the case with our enzyme.

Our measured dissociation constant of 64 μM obtained at pH 8.0 is somewhat larger than the value of 20 μM obtained at pH 7.2 by Wever et al. (1973) and close to the value of 50 μM found by Vygodina and Konstaninov (1985). While the former workers reported that the dissociation constant increases with pH, the latter workers found a bell-shaped dependence of K_d upon pH with the maximum occurring at pH 7.5. The value we find is actually smaller than that found by extrapolating Wever's data to pH = 8.0.

We find no change in the Soret MCD upon addition of azide, so that a high-spin to low-spin conversion of cytochrome a_3 of the kind promoted by cyanide has not occurred. On the other hand, there is a clear change in the MCD centered at 655 nm; this MCD feature reflects a porphyrin-to-iron charge-transfer (CT) transition and changes in this band implies some structural change at a_3. Nevertheless, unlike reaction with cyanide, this MCD band is not eliminated by azide and it would thus seem rather unlikely that there has been a change in spin state of cytochrome a_3 following azide binding.

Azide is also a ligand for copper. With model compounds in aqueous solvents the affinity is weak with dissociation constants ranging from 20 mM for neutral species to 7 mM for dipositive Cu; these values decrease markedly with a decrease in dielectric, and values less than 0.2 mM are found for dipositive copper in methanol (Casella et al., 1991). Formation of these copper complexes is usually associated with the appearance of weak absorption bands between 330 and 420 nm with intensities $A_m \sim 2500$ M^{-1} cm^{-1} (Pate et al., 1989; Casella et al., 1991). Pate et al. (1989) have analyzed the nature of the Cu(II)–N_3 absorption spectrum and associate these bands with a ligand-to-metal CT transition originating on the highest filled π^* orbital of azide and terminating on $d_{x^2-y^2}$ of Cu(II).

These CT transitions compete with the intrinsic heme absorbance of CcO present in the Soret region ($A_m \sim 160\,000$ M^{-1} cm^{-1}) and are consequently hard to detect directly, particularly if the azide reacts by displacing an endogenous imidazole copper ligand (His 46), as has been found with superoxide dismutase (Banci et al., 1989). However, these azide → copper CT have significant magnetic dipole character and are thus optically active. In the cases so far examined, the transitions exhibit a negative Cotton effect with ΔA_m falling in the range 1–9 M^{-1} cm^{-1} (Pate et al., 1989). The CD

spectrum of CcO in the Soret consists of a relatively intense positive Cotton effect centered at 428 nm with $\Delta A_m \sim 70\ M^{-1}\ cm^{-1}$. This optical activity arises from electronic coupling between π–π^* transitions occurring on the heme with π–π^* transitions on aromatic amino acids located close to and disposed dissymmetrically with respect to the heme (Hsu & Woody, 1971). Addition of 1 mM azide to CcO leads to a clear decrease in the intensity of the Soret CD spectrum; the difference spectrum is centered at 428 nm and has an amplitude of $-6\ M^{-1}\ cm^{-1}$. The sign and magnitude of this of change are consistent with azide binding to copper as exemplified by the data on met azide tyrosinase (Pate et al., 1989).

With the hope of further defining the interaction of azide with this enzyme we have turned to vibrational spectroscopy, for despite the practical difficulties associated with the technique, FTIR analysis of the binding of azide to CcO has the potential to provide direct information on the interaction of metal and ligand. Comparison of the frequency of the asymmetric stretch of azide bound to CcO with those of well-defined heme and copper proteins (Table I) indicates that the observed frequency is closest to that of a Cu(II)–N_3 species, the relevant values being 2056, 2061, and 2051 cm^{-1} for SOD (Table I; Blackburn et al., 1992), dopamine-β-hydroxylase (Blackburn et al., 1992) and CcO, respectively; these values are somewhat higher than those obtained with the two heme proteins, myoglobin and cytochrome *c* (Table I). However, the differences between the iron–azide and copper–azide frequencies are small and it would be imprudent to draw a firm conclusion on the location of the azide in CcO from such a limited data set.

Further insight into the mode of azide binding comes from a comparison of the behavior of azide and cyanide with CcO. Until recently it had been widely accepted that cyanide functions as a bridge between Cu_B and cytochrome a_3, a conclusion based on the observation that the presence of cyanide converts cytochrome a_3 to the low-spin state and substantially weakens the magnetic coupling to Cu_B, though the nature of this coupling is ambiguous with both the ferromagnetic (Thomson et al., 1981) and antiferromagnetic (Tweedle et al., 1978; Barnes et al., 1991) alternatives having been proposed.

The belief that cyanide occupied a bridging location at the binuclear center was recently challenged by Yoshikawa and Caughey (1990), who proposed that cyanide is bound to Cu_B. This conclusion was based in part on the finding that the stretching frequency of cyanide attached to CcO is at 2151 cm^{-1}, a finding that we have confirmed (Figure 7); this frequency was asserted to be inconsistent with a bridging location for cyanide. Additionally it was noted that one-electron-reduced CcO exhibited two peaks, at 2151 and 2131 cm^{-1}, in the presence of cyanide; it was assumed that one-electron enzyme completely lacked the presumed bridge between iron and copper and thus the 2151-cm^{-1} mode could not be due to cyanide in a bridging position. Finally, it was felt that the narrow line width of the observed IR mode was inconsistent with a bridging mode for cyanide.

We believe that none of these arguments survives scrutiny. First, for metal–cyanide complexes with 6 or less d-electrons, bonding to the metal ion is through carbon and tripositive metal ions typically give rise to a C–N stretch around 2130 cm^{-1} (Shriver et al., 1965). Metals with more than six d-electrons typically bind to cyanide through nitrogen; in this case dipositive metal ions exhibit a C–N stretch around 2130 cm^{-1} (Shriver et al., 1965). Pertinent biochemical examples would be Mb–cyanide (Yoshikawa et al., 1985) and superoxide dismutase–cyanide (Han et al., 1992) with cyanide stretching frequencies of 2126 and 2137 cm^{-1}, respectively. When cyanide is present as a bridge these frequencies are expected to increase by approximately 30 cm^{-1} (Shriver et al., 1965). Most mixed metal bridging cyanides exhibit cyanide stretches in the range 2100–2180 cm^- (Shriver et al., 1965), with one instance of a ferrous cupric cyanide bridge being observed at 2108 cm^{-1}; this frequency would be expected to be at ca. 2180 cm^{-1} in the ferric analog. Thus the infrared value of 2151 cm^{-1} found with CcO is clearly larger than that anticipated for either mononuclear copper or iron and is within reasonable range for that expected for cyanide coordinated as a Fe—C≡N—Cu species.

The presence of two cyanide stretches in one-electron-reduced CcO is readily explained. Cyanide-treated enzyme reduced with one electron has a composition which can be approximated as 40% cytochrome a^{2+} and 25% Cu_A^{1+} with the balance of the electron presumably on Cu_B, thus accounting for the finite amount of low-spin a_3–CN EPR signal which is detected (Garcia-Iniguez, 1980). Thus approximately 65% of the enzyme has the single electron present on either Cu_A or cytochrome *a*, and in this population of the enzyme cyanide can still occupy the bridging location. In the remainder of the enzyme the electron is present on Cu_B, the bridge is presumably broken, and cyanide becomes the distal ligand to the heme iron of cytochrome a_3. It thus appears that the mode at 2151 cm^{-1} reflects bridging cyanide while the mode at 2131 cm^{-1} is due to cyanide bound exclusively to the iron of a_3.

Furthermore as the possibilities for ligand disorder would appear to be much less in a bridging geometry, we find it more plausible to expect a bridging rather than a terminal cyanide to exhibit a narrow line width.

It thus seems that the original basis for concluding that cyanide is not a bridging ligand is not well founded. Indeed this conclusion appears to have been abandoned by Tsubaki and Yoshikawa (1991), though the basis for this change in position is not apparent from their paper.

We have now found that CcO pretreated with cyanide and subsequently incubated with equimolar azide does not exhibit an IR stretch at 2051 cm^{-1}, while CcO first treated with azide and then with cyanide loses the 2051-cm^{-1} mode; this latter result has also been obtained by Yoshikawa and Caughey (1992). The reaction proceeds with the normal red shift in the Soret band, the doubling in Soret MCD intensity, the loss of the 655-nm feature, and the red shift in the Soret CD and thus the reaction of cyanide with the enzyme appears to be normal.

This displacement of azide is most simply interpreted by assuming that cyanide and azide compete for the same site; the K_d of CcO for cyanide has been reported to be about 1 μM (Van Buuren et al., 1972), almost 100 times smaller than that of azide, so that cyanide should readily replace azide. However one cannot immediately rule out the alternative that cyanide and azide bind at different sites and that addition of cyanide labilizes the attachment of azide by something akin to a trans effect, although the data with thiocyanate (see below) make this unlikely.

One might have anticipated that cyanide could bind at two sites but this seems improbable as only one IR mode interpretable as a metal–cyanide stretch is observed (the feature at 2092 cm^{-1} seen in Figure 7 is due to the residual HCN present in the D_2O solvent). Thus the ability of cyanide to eliminate the IR stretch of bound azide is most simply interpreted as indicating that azide also occupies a bridging position.

This conclusion would appear to be inconsistent with the changes observed when ^{15}N azide is used as ligand. Analysis of the clearly broadened band (Figure 6) suggests that the splitting is of the order of 9 cm^{-1}, though the data are such that this value should be considered approximate. Previously Pate et al. (1989) have examined the mixed isotope splitting in a series of model copper complexes and shown that the splitting obtained with $^{15}N_3$ is between 6 and 11 cm^{-1} for terminally labeled azide (Cu–NNN), <2 cm^{-1} for μ-1,3-bridged azide derivatives (Cu–N–N–N–Cu), and greater than 17 cm^{-1} for μ-1,1-bridged derivatives. The value we find is clearly different from either of the two bridging geometries and thus nominally supports the assignment that azide is a terminal ligand to a metal, most plausibly Cu_B. The obvious alternative has azide coordinated to cytochrome a_3, trans to the proximal histidine and not bridging to Cu_B. In this configuration one would expect cytochrome a_3 to acquire substantial low-spin character. There is absolutely no evidence for any new low-spin species in either the EPR spectra or MCD spectra recorded in the Soret or near-infrared regions.

However, the interpretation of the isotope data is not as clear-cut as is first apparent. Raman data on azide binding to hemocyanin (Pate et al., 1986) show that the azide stretch at 2042 cm^{-1} splits into two lines, at 2023 and 2035 cm^{-1}, when the ^{15}N derivative is used. In this protein there is very good evidence that the azide is indeed present as a μ-1,3 bridge, and it was suggested by Pate et al. that the inequivalence in the two orientations of the bound ^{15}N-azide is a consequence of an asymmetric interaction of the ligand with the protein. In the same vein we suggest that the inequivalence in the two modes of binding of ^{15}N-azide to CcO are due to a difference in the N–N asymmetric stretch arising from Fe–N and Cu–N bonding, respectively; the electronic configurations of the d-orbitals of these two metal ions are completely different, and differences in bonding to the nitrogen are to be expected at the two metal centers.

Thus, while the spectroscopic data are most simply interpreted as indicating that azide is a terminal ligand to Cu_B, the ability of cyanide to block the binding of azide provides a strong indication that azide is in fact a bridge between these two metal centers. It should be noted that Yoshikawa and Caughey (1992) concluded that the IR mode at 2051 cm^{-1} was due to azide bound to a non-metal site in the fully oxidized enzyme. This conclusion was based on their inability to find a splitting in the presence of $^{15}N_3$ and on the presumption that such a splitting must necessarily exist when azide is bound to a metal. The study of Pate et al. (1989) shows that this presumption is not valid. As a crude test of whether a protein might cause nonspecific shifts in azide frequency, we examined a serum albumin–azide mixture by FTIR; no new bands were found. Yoshikawa and Caughey (1992) also observed a feature at 2041 cm^{-1} which they assigned to azide bound to Cu_B. This value is similar to that of 2039 cm^{-1} which we observe and have assigned as being due to azide bound to the heme of cytochrome *a*.

The conclusion that azide is a bridging ligand is supported by the results with thiocyanate. The affinity of CcO for SCN is about 50 times weaker than that for azide and it thus requires SCN concentrations of about 10 mM to approach saturation of the high-affinity SCN binding site. The observed decrease in absorbance is exceptionally small and the form of the changes is somewhat different than those found with azide; the marked inflection at 410 nm is replaced by a clearly resolved but very weak trough at 404 nm, while below 400 nm there is some evidence for a very weak and broad band centered at 360 nm. Interestingly, the wavelength and intensity of this band ($\Delta A_m \sim 300$ M^{-1} cm^{-1}) are very similar to the band at 360 nm, $\Delta A_m \sim 200$ M^{-1} cm^{-1}, which develops on addition of thiocyanate to superoxide dismutase (Dooley & McGuirl, 1986). SCN (10 mM) has almost no effect on the near-IR MCD at 655 nm or on the EPR of cytochrome *a* or of Cu_A.

Under these conditions we see a single C=N stretch at 2041 cm^{-1}, with position and width significantly less than that found with free thiocyanate (Table II). This band is about half as intense as that found with azide; the apparent structure is not reproducible and is attributed to decrease in the signal-to-noise ratio. The frequency of this C=N stretch is close to those found with thiocyanate complexes of myoglobin, cytochrome *c*, and superoxide dismutase (Table II) and consistent with bonding via nitrogen; S-bonding complexes are typically close to 2100 cm^{-1}. The strong similarity in frequency and the ^{15}N isotope shifts imply that thiocyanate is bound much the same in all four proteins. Coordination via nitrogen is the preferred behavior for metals of the first transition series.

Neither cyanide nor azide appear to compete for the thiocyanate binding site (Figures 9 and 10). This conclusion is strongest with cyanide, which has much the highest ligand affinity for the enzyme, but there is no reason to believe that it is not equally true with azide. Thus, given our assignment that cyanide and azide bind as bridging ligands, we are forced to conclude that SCN is bonded in a terminal mode to Cu_B, presumably through the nitrogen. This conclusion is consistent with the extremely small changes in the Soret absorbance, the Soret CD, and the 655-nm MCD transition induced by saturating thiocyanate and with the expectation that a bridging thiocyanate should exhibit a C=N stretch at 2100 cm^{-1} or higher (Nakamoto, 1986).

The inability of cyanide to displace thiocyanate suggests that the possibility for trans labilization suggested earlier is not present and that this potential mechanism for the displacement of azide by cyanide raised earlier can be discounted. Furthermore, it seems rather unlikely that azide and thiocyanate would simultaneously occupy terminal sites on Cu_B at the same time, as might otherwise be implied by the data of Figures 9 and 10.

The lack of an effect of SCN on the Soret CD is particularly telling because it implies that there has not been a significant change either in the optical characteristics of the heme or in the orientation of the heme with respect to its environment. It would be most unusual for SCN to bind to the heme of cytochrome a_3 and not affect one or the other of these two characteristics.

Thus the simplest way to reconcile our results is shown in Figure 11, with cyanide and azide occupying a bridging position between the heme iron of cytochrome a_3 and Cu_B while SCN occupies a second site located on Cu_B. This proposal leads to the idea that as many as three ligand binding sites might be available during the turnover of this enzyme, one on cytochrome a_3 and two on Cu_B. Two of these sites have been incorporated into several plausible mechanisms for the reduction of dioxygen and serve to stabilize the intermediates as they are formed [see, for example, Babcock and Wikstrom (1992)]. The role of the third site remains to be established, though there is at least one published mechanism which draws on ligand exchange reactions at Cu_B as the mechanism for proton translocation (Larsen et al., 1992).

The question now arises: if azide and cyanide both function as bridging ligands, why is it that only cyanide drives cytochrome a_3 to the low-spin state? The answer is to be found in the near-IR data of Thomson et al. (1985), who find

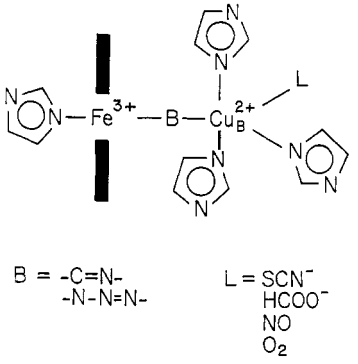

FIGURE 11: Proposal for the modes of ligand binding to oxidized cytochrome oxidase. The states of protonation of the histidines are left unspecified. B implies a bridging ligand between cytochrome a_3 and Cu_B, while L is a terminal ligand on Cu_B.

that a bridging cyanide is a weaker ligand than methionine with the near-IR MCD transition being located at 1946 nm. Given that cyanide is an intrinsically stronger field ligand than azide, it is not surprising that the ligand field strength of a bridging azide is insufficient to cause a high-spin to low-spin transition.

The proposal for the sites for ligand binding shown in Figure 11 throws into question our previous suggestion (Schoonover & Palmer, 1991) that the ability of formate to mimic the fast-to-slow transition is a result of formate blocking the now-discounted site of cyanide binding to Cu_B. A plausible alternative is that the binding of formate to Cu_B reduces the net charge on this metal and the less positive metal simply reacts more sluggishly with cyanide anion. As expected, we were unable to demonstrate an effect of formate on the FTIR of azide–CcO; estimates of the K_d for formate based on inhibition of catalytic activity are in the range 1–37 mM (Nicholls, 1975), much higher than that of either azide or cyanide.

The data with high concentrations of azide and SCN suggest that there are previously unsuspected complications with these reagents. High concentrations of azide clearly break an iron–histidine bond of cytochrome *a*, as evidenced by the changes in the EPR spectrum, and it is this reaction that is responsible for the optical changes in the Soret and the red shift in the near-infrared MCD occurring during the low-affinity phase. The Soret MCD is only slightly affected, presumably because one low-spin species is converted into a second low-spin species. The cytochrome *a*–N_3 adduct is responsible for the IR mode at 2039 cm^{-1}, some of which can already be detected during the high-affinity phase (Figure 6). This low-affinity phase for azide was also observed for cytochrome oxidase embedded in proteoliposomes (Vygodina & Konstantinov, 1985). With high concentrations of SCN the observed EPR changes are quite small and consist primarily of modifications to the EPR spectrum of Cu_A together with some loss in absorbance at 830 nm. There are some changes in the EPR envelope of the low-field peak of cytochrome *a*, but such changes are also seen with high concentrations of potassium chloride (Hartzell & Beinert, 1974) and most probably reflect an ionic strength effect. The difference in affinity of the two SCN binding phases is quite small, and concentrations of SCN as low as 20 mM are sufficient to produce some of the low-affinity species.

The reaction of azide with cytochrome *a* may explain some of the near-IR changes reported by Thomson et al. (1985), who found that 7 mM azide led to the formation of a new paramagnetic low-spin species under conditions in which the total low-spin content of enzyme did not change. This is the expected result if cytochrome *a* is modified as described above.

These latter data make it clear that the use of these and other ligands as probes of cytochrome oxidase structure and function should be restricted to the lowest concentration where specific effects can be demonstrated and stress the importance of examining the products of such reactions by as many techniques as is practical to be confident that unexpected side reactions have not occurred.

The spectral results obtained upon treating CcO with selenocyanate are puzzling. The optical and MCD changes are very similar to those obtained upon addition of cyanide and yet we can find no direct evidence for the presence of cyanide in our solutions. If this is true then it would appear that selenocyanate reacts differently than thiocyanate and is able to function in a bridging mode. Such a product should be most useful for an EXAFS study of the binuclear center.

ACKNOWLEDGMENT

We are indebted to Professor George J. Schroepfer Jr. for the generous and unrestricted access to his FTIR spectrometer and to Dr. W. Wilson for taking the time to instruct us in its use.

REFERENCES

Alben, J. O., Moh, P. P., Fiamingo, F. G., & Altschuld, R. A. (1981) *Proc. Natl. Acad. Sci. U.S.A. 78*, 234–237.

Babcock, G. T., & Wikstrom, M. (1992) *Nature 356*, 301–309.

Babcock, G. T., Vickery, L. E., & Palmer, G. (1976) *J. Biol. Chem. 251*, 7907–7919.

Baker, G. T., Noguchi, M., & Palmer, G. (1987) *J. Biol. Chem. 262*, 595–604.

Banci, L., Bertini, I., Luchinat, C., & Scozzafava, A. (1989) *J. Biol. Chem. 264*, 9472–9744.

Barnes, Z. K., Babcock, G. T. & Dye, J. L. (1991) *Biochemistry 30*, 7597–7603.

Blackburn, N. J., Reedy, B., Zhou, E., Carr, R., & Benkovic, S. J. (1992) *J. Inorg. Biochem. 47*, 8.

Blumberg, W. D., & Peisach, J. (1971) in *Bioinorganic Chemistry* (Dessy, R., Willard, J., & Taylor, L., Eds.) Advances in Chemistry Series, Vol. 100, pp 271–291, American Chemical Society, Washington, DC.

Brudvig, G. M., Stevens, T. H., Morse, R. H., & Chan, S. I. (1981) *Biochemistry 20*, 3912–3921.

Casella, L., Gullotti, M., Pallanza, G., & Buga, M. (1991) *Inorg. Chem. 30*, 221–227.

Caughey, W. S. (1980) in *Methods for Determining Metal Ion Environments in Proteins: Structure and Function of Metalloproteins* (Darneall, D. W., & Wilkins, R. G., Eds.) pp 95–115, Elsevier, New York.

Dooley, D. M., & McGuirl, M. A. (1986) *Inorg. Chem. 25*, 1261–1264.

Garcia-Iniquez, L. (1980) Oxidative–reductive Intermediates of Cytochrome Oxidase, Ph.D. Thesis, Rice University, University Microfilms, Ann Arbor, MI, Access No. 80-18053.

Gelles, J., Blair, D. F., & Chan, S. I. (1986) *Biochim. Biophys. Acta 853*, 205–236.

Han, J., Blackburn, N. J., & Loehr, T. M. (1992) *Inorg. Chem. 31*, 3223–3229.

Hartzell, C. R., & Beinert, H. (1974) *Bichim. Biophys. Acta 368*, 318–338.

Hsu, M., & Woody, R. W. (1971) *J. Am. Chem. Soc. 93*, 3515–3525.

Ikeda-Saito, M., & Iizuka, T. (1975) *Biochim. Biophys. Acta 393*, 335–342.

Larsen, R. W., Pan, L., Musser, S. M., Li, Z., & Chan, S. I. (1992) *Proc. Natl. Acad. Sci. U.S.A. 89*, 723–727.

McCord, J. M., & Fridovich, I. (1969) *J. Biol. Chem. 244*, 6049–6055.

Mitchell, R., Mitchell, P., & Rich, P. R. (1991) *FEBS Lett. 280*, 321–324.
Myer, Y. P. (1971) *J. Biol. Chem. 246*, 1241–1248.
Nakamoto, K. (1986) in *Infrared and Raman Spectra of Inorganic and Coordination Compounds*, 4th ed., John Wiley & Sons, New York.
Nicholls, P. (1975) *Biochem. Biophys. Res. Commun. 67*, 610–616.
Nicholls, P., Petersen, L. C., Miller, M., & Hansen, F. B. (1976) *Biochim. Biophys. Acta 449*, 188–196.
Palmer, G. (1985) *Biochem. Soc. Trans. 13*, 548–560.
Pate, J. E., Thamann, T. J., & Solomon, E. I. (1986) *Spectrochim. Acta 42A*, 313–318.
Pate, J. E., Ross, P. K., Thamann, T. J., Reed, C. A., Karlin, K. D., Sorrell, T. N., & Solomon, E. I. (1989) *J. Am. Chem. Soc. 111*, 5198–5209.
Schoonover, J. R., & Palmer, G. (1991) *Biochemistry 30*, 7541–7550.
Shriver, D. F., Shriver, S. A., & Anderson, S. E. (1965) *Inorg. Chem. 4*, 725–730.
Sono, M., & Dawson, J. H. (1982) *J. Biol. Chem. 257*, 5496–5502.
Thomson, A. J., Johnson, M. K., Greenwood, C., & Gooding, P. E. (1981) *Biochem. J. 193*, 687–697.
Thomson, A. J., Greenwood, C., Gadsby, P. M. A., Peterson, J., Eglington, D. G., Hill, B. C., & Nicholls, P. (1985) *J. Inorg. Biochem. 23*, 187–197.
Tsubaki, M., & Yoshikawa, S. (1991) in *Spectroscopy of Biological Macromolecules* (Hester, R. E., & Girling, R. B., Eds.) pp 269–270, The Royal Society of Chemistry, London.
Tweedle, M. F., Wilson, L. J., Garcia-Iniguez, L., Babcock, G. T., & Palmer, G. (1978) *J. Biol. Chem. 253*, 8065–8071.
Van Buuren, K. J. H., Nicholls, P., & Van Gelder, B. F. (1972) *Biochim. Biophys. Acta 256*, 258–276.
Vickery, L., Nozawa, T., & Sauer, K. (1976) *J. Am. Chem. Soc. 98*, 351–357.
Vygodina, T. V., & Konstantinov, A. A. (1985) *Biol. Membr. 2*, 861–869 (USSR, Russian ed.).
Wever, R., Muijsers, A. O., Van Gelder, B. F., Bakker, E. P., & Van Buuren, K. J. H. (1973) *Biochim. Biophys. Acta 325*, 1–7.
Wikstrom, M. (1989) *Nature 338*, 776–778.
Woodruff, W. H., Einarsdottir, O., Dyer, R. B., Bagley, K. A., Palmer, G., Atherton, S. J., Goldbeck, R. A., Dawes, T. D., & Kliger, D. S. (1991) *Proc. Natl. Acad. Sci. U.S.A. 88*, 2588–2592.
Yoshikawa, S., & Caughey, W. S. (1982) *J. Biol. Chem. 257*, 412–420.
Yoshikawa, S., & Caughey, W. S. (1990) *J. Biol. Chem. 265*, 7945–7958.
Yoshikawa, S., & Caughey, W. S. (1992) *J. Biol. Chem. 267*, 9757–9766.
Yoshikawa, S., O'Keeffe, D. H., & Caughey, W. S. (1985) *J. Biol. Chem. 260*, 3518–3528.